Analyst

Accepted Manuscript

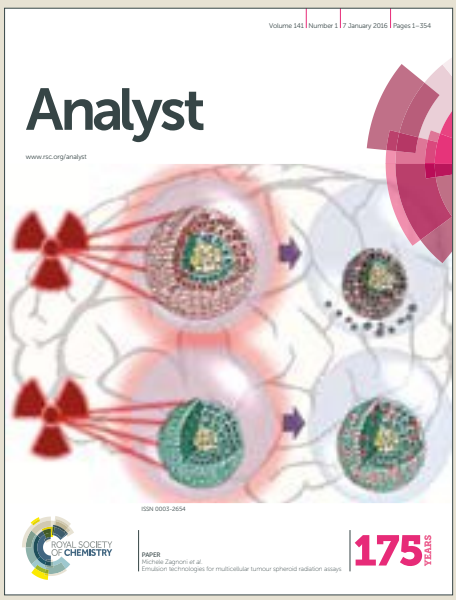

ROYAL SOCIETY OF CHEMISTRY

rsc.li/analyst

Analyst

View Article Online
DOI: 10.1039/C8AN00567B

ARTICLE

Rapid and sensitive detection of nodularin-R in water by a label-free BLI aptasensor

Received 00th January 20xx,
Accepted 00th January 20xx

DOI: 10.1039/x0xx00000x

www.rsc.org/

Shengqun Ouyang † [a] , Bo Hu † [a], Rong Zhou † [a], Dejing Liu[a], Dingfa Peng[a], Zhengang Li[a,b], Zhen Li[a], Binghua Jiao*[a,b], Lianghua Wang* [a]

Contamination of freshwater with nodularin-R (NOD-R) represents significant global environmental and public health concerns. However, ethical problems and technical difficulties surrounding current detection methods for NOD-R necessitate further studies to devise appropriate alternatives within a regulatory monitoring regime. In this work, we employed an aptamer as the specific recognition element and developed a biolayer interferometry (BLI) biosensor platform for NOD-R detection. The aptasensor we propose displayed a broad detection range from 40 to 600 nM NOD-R (and linear range response from 40 to 200 nM), and achieved a detection limit as low as 167 pM. In addition, the aptamer-based biosensor was shown to possess high selectivity, as well as good reproducibility and stability. We believe that this novel aptamer-based biosensor provides a potential alternative for the sensitive and rapid detection of NOD-R.

1. Introduction

Cyanophycean, a famous blue-green prokaryote, can form blooms in water and generate toxins known as cyanophycean toxins. These toxins are of diverse chemical nature and are mainly classified into hepatotoxins, neurotoxins and dermatotoxin [1]. When blooms occur, hepatotoxins are the most frequently detected toxic molecules and are most often implicated in intoxication cases. Nodularins (NODs), cyclic peptides composed of five amino acids, are among the three most common hepatotoxins produced by cyanophyceans. Since first being described in 1988 [2], approximately ten variants have been discovered. Among the forms of NOD, NOD-R is the most abundant, and the only commercially available (Fig. S1). The toxicity of NODs is related to the inhibition of the catalytic subunits of serine/threonine-specific protein phosphatases (PPs) 1 and 2A (PP1 and PP2A) [3]. NODs are water soluble and heat stable, so they cannot be completely eliminated via routine water treatment processes. Humans may be exposed to NODs through the consumption of contaminated drinking water or via skin contact at recreational sites. A guideline value of 1 μg/L of NODs in drinking and recreational water has been suggested based on toxicity studies [4]. This regulation regime requires rapid and sensitive detection methods for NODs.

The mouse bioassay (MBA) is a widely used method for estimating the toxicity of cyanophycean toxins, including NODs [5]. However, poor specificity and sensitivity, as well as ethical concerns, have hindered more widespread adoption of this method. Analytical methods, such as high-performance liquid chromatography (HPLC), liquid chromatography coupled with mass spectrometry (LC-MS), and capillary electrophoresis (CE), have been applied recently [6-9]. However, these techniques are time-consuming, costly, and not suitable for on-site detection. On the other hand, immunological methods have been established for NODs detection [10, 11], including enzyme linked immunosorbent assay (ELISA) methods. However, these techniques are usually expensive and complicated, and leave open the possibility of cross-reactions. Taken together, these methods cannot meet the demands related to the accurate and rapid detection of NODs. Biosensors are good alternatives for the monitoring of cyanophycean toxins, because they avoid most of the disadvantages of other methods. The core component of a biosensor is a molecular recognition element. Antibodies are ideal recognition elements, but they are usually expensive and can denature easily, requiring special storage conditions. Thus, there is still an urgent need to develop a novel probe that is economical and convenient, as well as highly specific and sensitive to NODs.

Aptamers are functional single stranded DNA (ssDNA) or RNA oligonucleotides obtained from the Systematic Evolution of Ligands by Exponential Enrichment (SELEX) method, an in vitro evolution-like process [12, 13]. Aptamers offer almost all the advantages of antibodies, while also provide unique features [14]. For example, they can be synthesized using a well-established, automated solid-phase synthesis process in a simple, fast, and cost-effective manner. They can recognize a large variety of targets, such as small molecules, proteins, and cells, and can be modified easily by various functional tags to induce

[a] Department of Biochemistry and Molecular Biology, College of Basic Medical Sciences, Second Military Medical University, Shanghai 200433, China.
[b] Marine Biological Institute, College of Marine Military Medicine, Second Military Medical University, Shanghai 200433, China.
† Co-first authors.
* Correspondence authors: Binghua Jiao, Lianghua Wang.
Electronic Supplementary Information (ESI) available: See DOI: 10.1039/x0xx00000x

View Article Online
DOI: 10.1039/C8AN00567B

immobilization onto many surfaces. Finally, aptamers are thermally stable enough to be shipped commercially at ambient temperatures. As a novel molecular recognition element, aptamers have attracted increasing attention in aptasensors construction. Many aptasensors targeting cyanophycean toxins have previously been reported, including for saxitoxin [15, 16], gonyautoxin 1/4 [17], anatoxin-a [18], cylindrospermopsin [19, 20] and microcystin-LR [21, 22]. Aptamers can be employed in different types of biosensors [17, 23-30], including surface plasma resonance (SPR), quartz crystal microbalances (QCM), electrochemical methods, colorimetric methods, or biolayer interferometry (BLI). As a label-free, real-time and highly sensitive optical biosensor, BLI-based biosensors have been rapidly developed in recent years [31, 32]. We report the first BLI aptasensor for gonyautoxin 1/4 detection [17], In addition, we constructed a palytoxin aptamer-based BLI biosensor [27]. There have been no previous reports of aptamer selection and identification for NOD-R, and certainly not for aptasensor applications. Here, we report the first successful selection, characterization and BLI biosensor application of a DNA aptamer that binds specifically and tightly to NOD-R.

2. Materials and methods

2.1 Materials and reagents

Nodularin-R (NOD-R), microcystin-LR (MC-LR), palytoxin (PTX), brevetoxin (BTX), gonyautoxin (GTX), and saxitoxin (STX) were purchased from Taiwan Algal Science, Inc. (Taiwan). 2-(N-morpholino)-ethanesulfonic acid (MES), 1-Ethyl-3-(3-dimethylaminopropyl) carbodiimide hydrochloride (EDC), N-hydroxysuccinimide (NHS), and the other chemical agents were procured from Sigma-Aldrich Co. LLC (Mainland, China). Dynabeads® M-270 Amine and the Qubit® ssDNA Assay Kit were obtained from Thermo Fisher Scientific (Massachusetts, USA). GoTaqHot® Start Colorless Master Mix was purchased from the Promega Corporation (Wisconsin, USA). Oxalic acid (ultra-pure grade) was procured from BBI Life Sciences Corporation (Shanghai, China). The QIAEX® Ⅱ Gel Extraction Kit was obtained from Qiagen (Frankfurt, Germany). The 20 bp DNA Ladder (Dye Plus) was purchased from TaKaRa Bio, Inc. (Dalian, China). Bio Gel P-2 was procured from Bio-Rad (Hercules, USA). Urea (ultra-pure grade) was obtained from Amresco, Inc. (Ohio, USA). The BLI sensor chips were purchased from Forte Bio (Shanghai, China). DNA Urea-PAGE buffer, DNA PAGE buffer and binding buffer (pH 7.5, 50 mM Tris-HCl, 150 mM NaCl, 2 mM $MgCl_2$) were procured from Tiandz (Beijing, China). Binding buffer was used for aptamer selection and the biolayer interferometry (BLI) experiment. The elution buffer was consisted of the binding buffer and 7 mM urea. All nucleic acid sequences were custom synthesized by Sangon Biotech Co. Ltd (Shanghai, China). All solutions were prepared using Milli-Q ultrapure water.

2.2 Preparation of magnetic beads coupled with NOD-R

Lyophilized NOD-R (10 μg) was dissolved in 100 μL MES buffer (25 mM, pH 5). Similarly, 50 mg EDC and 50 mg of NHS were dissolved in 1 mL MES buffer. Then, the NOD-R solution was mixed with the above 50 mg/mL EDC and NHS solutions. After incubation for 30 min with slow tilt rotation (BE-1100, the rotating speed is 18 RPM) at room temperature, 400 μL amine beads (Dynabeads® M-270 Amine, cat. no. 14307D), which were washed four times with MES buffer, were added for a total volume of 1.5 mL. The mixture was rotated slowly at room temperature. After two hours, the beads were washed four times with MES buffer to discard the unreacted NOD-R. Next, 500 μL 0.5 M oxalic acid was added to block any unreacted amino groups existing on the surface of amine beads. As before, 50 mg of EDC and 50 mg of NHS were dissolved in 1 mL MES buffer and incubated with oxalic acid for 30 min with slow tilt rotation at room temperature. After incubation, 1000 μL of the mixture was added to 400 μL of the NOD-R coated beads. The remaining 500 μL of the mixture was incubated with 200 μL of the washed amine beads for negative selection. After an additional 2 hours of end-over-end rotation at room temperature, the beads were washed extensively with the binding buffer. Finally, 400 μL and 200 μL binding buffer were added into the NOD-R coated beads and negative beads, respectively. And they were stored at 4 °C before application.

2.3 Random ssDNA library and primer set

A random ssDNA library containing 3nmol ssDNA oligonucleotides was chemically synthesized and purified by Sangon Biotech Co. Ltd. The ssDNA library sequences were consisted of a central region of 40 random nucleotides and 20 fixed nucleotides at both the 3' and 5' ends. The library sequence was: 5'- AAGGAGCAGCGTGGAGGATA-N40-TTAGGGTGTGTCGTCGTGGT-3' (80-mer). The fixed nucleotides were primer binding sites for the amplification of the library sequences. The forward primer was: 5'-AAGGAGCAGCGTGGAGGATA-3'; and the two reverse primers were A: 5'-ACCACGACGACACACCCTAA-3'; and B: 5'-AAAAAAAAAAAAAAAAAAAA-Spacer18-ACCACGACGACACACCCTAA-3'. The unmodified reverse primer was used for PCR amplification and cloning when SELEX was performed. The modified reverse primer was designed for the separation of target ssDNA from the PCR-amplified double stranded DNA.

2.4 In vitro selection of the DNA aptamers

Magnetic bead-SELEX (MB-SELEX), the classic SELEX technique employing magnetic beads to immobilize target molecules, was conducted to select aptamers against NOD-R. The MB-positive and MB-counter SELEX processes are illustrated in Fig. 1A, following the protocol detailed in Table S1. A certain amount of ssDNA oligonucleotides (3 nmol in the first selection round; 200 pmol in the second to the fifth selection rounds and 120 pmol in the subsequent selection rounds) were dissolved in binding buffer. Before selection, the samples were heated at 95 °C for 10 min, cooled in an ice bath for 5 min and kept at room temperature for 5 min to assure optimal structural conformation. At the same time, the NOD-R beads were washed several times with binding buffer. The prepared library and 20 μL washed NOD-R beads were immediately added into a microcentrifuge tube. Binding buffer was added

View Article Online
DOI: 10.1039/C8AN00567B

to obtain a total volume of 600μL. After incubating the mixture with end-over-end rotation at room temperature, the beads were washed several times with 600 μL binding buffer until no ssDNA could be detected in the supernatant. The ssDNA bound to the NOD-R beads was eluted with 80 μL elution buffer three times with shaking and heating at 95 °C for 20 min. The eluted ssDNA was quantified using a Qubit® 2.0 fluorometer, amplified by PCR, and purified using a gel extraction kit. For the MB-counter SELEX, the ssDNA library, subjected to the same heating and cooling treatment as before, was incubated with the negative beads. The ssDNA in the supernatant was then recovered and quantified. After another round of heating and cooling treatment, the ssDNA was incubated with NOD-R beads. After incubation at room temperature, the NOD-R beads were washed and eluted as before. The eluted ssDNA was quantified using a Qubit® 2.0 fluorometer, amplified by PCR, and purified using a gel extraction kit.

2.5 Amplification and purification of the DNA aptamers

The enriched pools were amplified using PCR in 40 parallel 50 μL reactions, each containing Go Taq® Hot Start DNA Polymerase and Colorless Go Taq® Reaction Buffer (pH 8.5), 200 μM dNTP, 2 mM MgCl2, and 0.5 μM forward and reverse primer B. The PCR conditions were: 95 °C for 5 min, followed by 25 cycles of 95 °C for 30 s, 62 °C for 45 s, 72 °C for 30 s, and a final elongation step of 5 min at 72 °C. The enriched ssDNA in the PCR products was separated using 12% urea denaturing PAGE, and recovered by boiling the gel band. The eluted ssDNA in binding buffer was collected and purified using a gel extraction kit. Finally, the purified ssDNA was quantified using a Qubit® 2.0 fluorometer and applied in the next selection round.

2.6 Cloning and sequencing of the selected DNA aptamers

After 12 rounds of selection, the ssDNA pool selected by the MB-SELEX processes was amplified with the forward and reverse primer A (unmodified reverse primer). The PCR products were purified using a gel extraction kit. The collected double stranded DNA was cloned and sequenced by Sangon Biotech Co. Ltd. The target ssDNA sequences were aligned and analyzed by the Clustal X 2.1 software. Their secondary structures were predicted by the mfold web server (http://unafold.rna.albany.edu/?q=mfold).

2.7 Determination of affinity and specificity of aptamer using BLI

The affinity and specificity of the aptamer were determined via BLI using an OctetRED 96 system (ForteBio, Shanghai). The principle of operation and analysis procedures are described in Concepcion et al [33]. As shown in Fig. S4, the assay procedure included five steps: baseline (2 min), loading (5 min), washing (3 min), association (5 min), and dissociation (5 min). The baseline solution (200 μL, pH 7.5, 50 mM Tris-HCl, 150 mM NaCl, 2 mM MgCl2), loading solution (i.e. baseline solution), washing solution (i.e. baseline solution), association solution (i.e. baseline solution) and dissociation solution (i.e. baseline solution) were added, respectively, into the corresponding wells of a 96-well microtiter plate. All the steps were performed at room temperature with shaking at 1000 RPM in the 96-well microtiter plate. To eliminate non-specific binding and buffer-induced interferometry spectrum shifts, we normalized the response data obtained from the reaction surface by subtracting the signal acquired from the control surface using the Octet Data Analysis Software CFR Part 11 Version 6.x. The affinity parameter K_D was obtained in this way, and a 1:1 binding mode with mass transfer fitting was applied to obtain the kinetic data.

2.8 BLI aptasensor preparation

A super streptavidin-coated (SSA) biosensor was used for the immobilization of the NOD-R aptamer onto the BLI aptasensor. The online preparation of SSA aptasensor included three steps: sensor activation (2 min), biotin modified aptamer immobilization (5 min), and (3) washing (3 min). The aptasensor responses obtained from the reaction surface were also corrected by subtracting the signal acquired from the control surface to eliminate the effects of non-specific binding and any buffer-induced interferometry spectrum shifts.

3. Results and discussion

3.1 In vitro selection of the DNA aptamers

Before conducting the in vitro selection, we quantified the unreacted NOD-R using an ELISA kit. And obtained the efficiency of immobilization (52%). It means that the final concentration of coated NOD-R (MW=825) was 15 pmol/uL. The MB-SELEX process, including positive and counter selection, is illustrated
in Fig. 1A, following the protocol detailed in Table S1. To improve the screening efficiency, the size of the ssDNA pool,

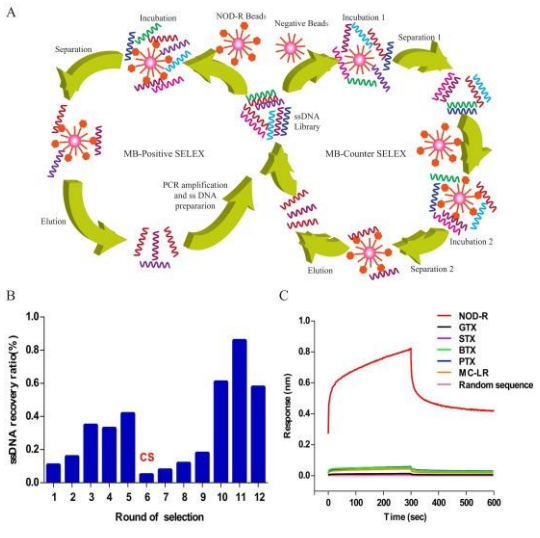

Fig. 1 (A) Processes of MB-positive SELEX and MB-counter SELEX. (B) Recovery ratio of ssDNA during MB-SELEX. (C) Characterization of affinity and specificity of aptamer N13-T-O2 for NOD-R. The red line represents the interaction curve of aptamer N13-T-O2 with NOD-R. The dark purple, light purple, green, blue, and yellow lines represent the interaction curves

View Article Online
DOI: 10.1039/C8AN00567B

of aptamer N13-T-O2 with GTX, STX, BTX, PTX and MC-LR, respectively. The pink line represents the interaction curve of a random sequence with NOD-R.

incubation time, and wash times after incubation were altered during the selection process. In addition, negative beads were introduced to remove the ssDNA that bound non-specifically to the magnetic beads, starting with round 6. After 12 rounds of selection, the ssDNA recovery ratio reached a plateau, and showed no more significant increases (Fig. 1B), at which point we stopped the selection cycles.

In all, we identified 80 sequences. Multiple sequence alignment was performed using Clustal X 2.1 software. As a result, we grouped these sequences based on conservation into 10 families (A-J) (Fig. S2). Then, we predicted the secondary structures of these sequences using the mfold web server. The sequence with the highest homology, or minimum free energy, in each group was chosen for further binding affinity studies with NOD-R, as shown in Table S2. Among all the sequences selected from each group, seven sequences exhibited binding affinity to NOD-R, ranging from 0.138 to 14.3 μM, while three sequences showed no binding. In addition, sequence N13 showed the highest binding affinity (0.138 μM) and was used for further study.

3.2 Truncation of aptamer N13

Apart from the selection process, we also optimized aptamer N13, which displayed the lowest K_D value. Truncated sequences of aptamer N13 are given in Table S3. Their secondary structures predicted by the mfold web server are shown in Fig S3. After the primer binding sites at each end of N13 were truncated (N13-T), the aptamer not only retained the capability to bind to NOD-R, but even exhibited equivalent affinity. This means that primer binding sites were not essential for the interaction between aptamer N13 and NOD-R. As a result, we further truncated N13-T based on the prediction of the mfold web server, and obtained variants N13-T-O1, N13-T-O2, N13-T-O3, and N13-T-O4. All of these aptamers displayed considerable affinity to NOD-R, except for N13-T-O4. Based on the secondary structures of N13-T-O1, N13-T-O2, N13-T-O3, and N13-T-O4, we speculate that the larger stem loop is the core sequence for NOD-R binding. Also, nucleotides along with the larger stem loop are critical for higher binding affinity. In light of the expense in time and money, we did not truncate nucleotides one by one to find the optimal number with respect to the highest binding affinity. In other words, we suppose that N13-T-O2, whose binding affinity is the highest, is the best sequence for NOD-R. After truncation, the K_D value decreased from 138 to 29.6 nM.

3.3 Determination of the affinity and specificity of aptamer N13-T-O2 using BLI

As shown in Fig. 1C, 1 μM NOD-R was analyzed for association and dissociation, along with 10 μM GTX, STX, BTX, PTX, and MC-LR as non-specific targets. Among the five toxins, GTX and STX are alkaloids, while BTX and PTX are polyethers. MC-LR, the analog of NOD-R, is a peptide. In addition, a random sequence was applied as an aptamer control. Also, a blank sample containing only the running buffer was used for reference. The results revealed that NOD-R interacted with N13-T-O2 with a K_{on} (1/Ms) value of 5.44E+04, a K_{dis} (1/s) value of 1.61E-03, and a K_D (M) value of 2.96E-08. In addition, GTX, STX, BTX, PTX and MC-LR showed almost no response (Fig. 1C), which revealed that N13-T-O2 exhibited specific binding to NOD-R. Meanwhile, the random sequence showed no binding to NOD-R, which demonstrated that NOD-R bound to N13-T-O2 only. These results indicate that aptamer N13-T-O2 binds to NOD-R with high affinity and specificity.

3.4 BLI aptasensor for NOD-R detection

The aptamer N13-T-O2 was further used to construct a real-time, label-free optical BLI aptasensor. As an innovative and powerful biosensor platform, BLI uses biolayer interferometry technology to monitor variations in the interfacial properties at the sensor surface when the immobilized ligands bind to the target molecules [34]. As shown in Fig. 2A, when aptamers were immobilized on the surface of the sensor, the binding of NOD-R to the sensor surface caused a shift in the interference spectrum. The wavelength shift (Δλ, Fig. 2A) reflects changes in the optical thickness and mass density of the sensor layer, which is recorded as a change in wavelength as a function of time. Only when the target molecule, NOD-R, became bound to, or dissociated from, the biosensor surface did the interference spectrum change. This allowed response curves to be generated. As a characteristic spectral signature, the interference was captured and reported in relative intensity units. The SSA biosensor is optimal for the analysis of small molecules [17]. In this study, more aptamers could be immobilized on the SSA sensor chip. Therefore, we chose a SSA biosensor for the immobilization of aptamer N13-T-O2 onto the aptasensor. The procedure for BLI-based detection included three steps. As shown in Fig. 2B, in the first step of the assay, the prepared SSA biosensor was submerged for 3 min in the binding buffer. The biosensor was then incubated with samples containing NOD-R for 5 min. Finally, the NOD-R bound to the biosensor surface gradually dissociated from the streptavidin-biotin-aptamer-NOD-R complex and dissolved into the binding buffer.

In order to take the newly developed BLI aptasensor for NOD-R detection into practice, we assessed the properties of

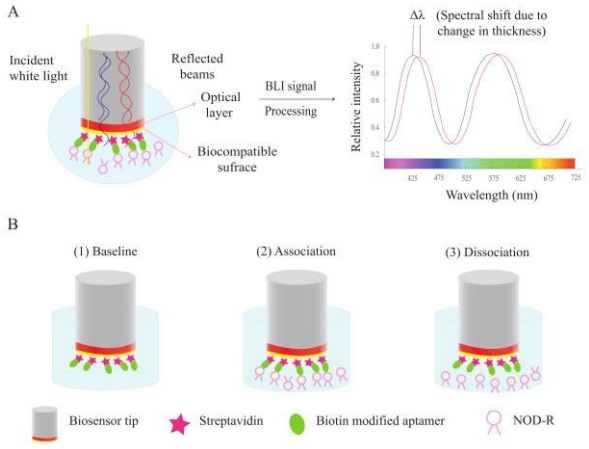

View Article Online
DOI: 10.1039/C8AN00567B

this biosensor. The real-time responses of NOD-R at different

Fig. 2 (A) Principle of the BLI-based NOD-R detection system. (B) Schematic of the working principles of the BLI aptasensor.

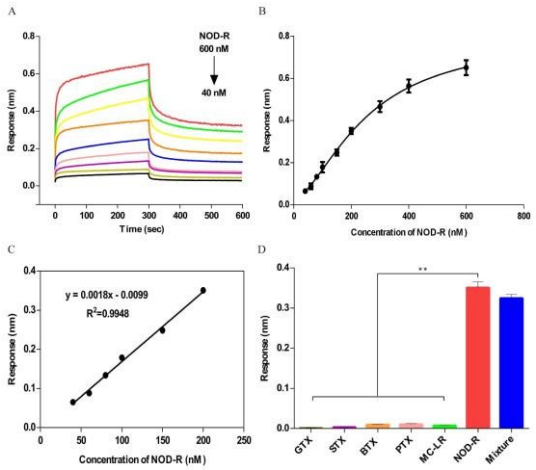

Fig. 3 (A) Response plot for the aptamer-based BLI biosensor after addition of NOD-R at different concentrations (40-600 nM). (B) The calibration curve for NOD-R from 40 to 600 nM, a plot of the response as a function of the NOD-R concentration. The error bars represent standard deviations. (C) The linear range of the calibration curve for NOD-R, a plot of the response as a function of the NOD-R concentration from 40 to 200 nM. (D) Specificity of the aptasensor with GTX, STX, BTX, PTX, MC-LR, and NOD-R (each at 200 nM), and the mixture (NOD-R at 200 nM, and the other toxins each at 10 μM), respectively. The error bars represent standard deviations. **p < 0.01, vs NOD-R (control)

concentrations, ranging from 40 to 600 nM, were observed. As a result of the greater density and thickness changes at the biolayer surface, the BLI response was enhanced at increasing NOD-R concentrations (Fig. 3A). With each sample repeated in duplicate, a calibration curve of the BLI response at 300 s as a function of the NOD-R concentration was obtained (Fig. 3B). The curve was fitted to a sigmoidal logistic four-parameter equation:

$y = (R_{max} - R_{min}) / [(1 + (x/EC_{50}) \text{ ^}b)] + R_{min}$. Here, Rmax and Rmin are the maximum and minimum responses of the curve, respectively. EC50 is the NOD-R concentration resulting in half of the maximum response, while b stands for the correction factor. After collection of the experimental data, we found the following relation: y= (0.8025- 0.0280)/[1+(x/250.7)^-1.643]+ 0.0280. The correlation coefficient R2 was 0.9911. In addition, the aptasensor showed a linear detection range between 40 and 200 nM NOD-R, which can be expressed by the linear regression equation: y = 0.0018x - 0.0099. As shown in Fig. 3B, the regression coefficient of the linear plot is 0.9948. The limit of detection (LOD, 167 pM) was calculated following the International Union of Pure and Applied Chemistry (IUPAC): 3 standard deviations of the response induced in the absence of NOD-R and sensitivity of the linear calibration graph. Moreover, the reproducibility of the aptasensor was evaluated by measuring the signal after the addition of 100 nM NOD-R eight times. The coefficient of variation (CV) was 8.23%, which indicates that the aptasensor possessed good reproducibility.

High specificity is an essential property for the aptasensor, especially when detecting samples in complex environments. Cross-reactivity experiments were conducted in duplicate with 200 nM GTX, STX, BTX, PTX, and MC-LR. As shown in Fig. 3C, NOD-R caused a response of 0.35 nm, while the other toxin samples caused responses of less than 0.01 nm. Furthermore, a mixture containing 200 nM NOD-R and the other toxins (each at 10 μM, 50 times higher than NOD-R) caused a response of 0.32 nm, which was comparable to when only NOD-R is present. These results show that the aptasensor can be used to detect NOD-R with high sensitivity, even in an environment with different kinds of toxins.

Comparative study between the reported aptasensors for other cyanophycean toxins and the proposed aptasensor for NOD-R was performed. As displayed in Table 1, the linear range of the aptasensor developed in this work is poorer than the reported aptasensors. However, the new aptasensor exhibits superior or equal limit of detection.

Although the existing methods (HPLC: 0.04 μg/L [6], ELISA: 0.042 μg/L [11], and CE-MS: 0.014 μg/L [9]) have lower detection limits, the LOD (0.138 μg/L) acquired here is apparently below the guideline value for NOD-R (1 μg/L). Therefore, the aptasensor is still prospective for NOD-R detection. What's more, the novel detection technique possesses some merits compared with traditional ones. Firstly, the approach is consisted of simple procedures and requires no professional skills. What we should do is immobilizing the biotin modified aptamer onto the surface of the biosensor. Secondly, the whole detection could be completed within 15 minutes, which is more efficient than other methods. Thirdly, the expense of the technique is much cheaper. On the one hand, aptamer and biosensor are cost-effective. On the other hand, aptamer modified biosensor can be reused after regenerating with washing buffer for approximately 180s. Last but not the least,

Table 1 Comparison of various aptasensors for cyanophycean toxins detection

Analytical techniques	Targets	Linear range	LOD	Reference
BLI	Saxitoxin	0.33-2.68μM	1.67 nM	16
Electrochemical	Saxitoxin	0.9-30 nM	0.38 nM	15
BLI	Gonyautoxin1/4	0.51-228 nM	127 pM	17
Electrochemical	Anatoxin-a	1 nM-100 nM	0.5 nM	18
Electrochemical	Cylindrospermopsin	0.1-80 nM	100 pM	19
Electrochemical	Cylindrospermopsin	0.93-188 nM	282 pM	20
BLI	Nodularin-R	40-200 nM	167 pM	This work
Microcantilever	Microcystin-LR	1–50 nM	1 nM	35
Fluorescence	Microcystin-LR	0.4-1200	138	36

Colorimetry	Microcystin-LR	nM 0.0005- 7.5 μM	pM 0.37 nM	37

Table 2 Recovery studies of tap water with different concentration of NOD-R (n=3).

Tap water	NOD-R (nM)	Recovery (%)	CV (%)
1	50	102.16	3.73
2	80	91.92	3.22
3	100	94.85	1.31

Note: The tap water experiments were all conducted with processed tap water (supplied with one tenth of 10 × concentrated binding buffer).

the method exhibited high specificity, meaning that the aptasensor identify NOD-R only. Consequently, we propose that the aptasensor has the potential to be an alternative for routine NOD-R detection.

3.5 Detection of NOD-R in Tap Water

To evaluate the usefulness of the newly developed BLI aptasensor with a real sample, tap water with different concentration of NOD-R was studied. As shown in Table 2, a good recovery percentage of 91.92 to 102.16% was obtained. Meanwhile, no significant interference from the tap water on the aptasensor operation was observed, and the CV value was acceptable. As a result, we can conclude that the BLI aptasensor possesses the potential to be used for the detection of NOD-R in real samples.

4. Conclusion

In summary, we constructed a BLI aptasensor for NOD-R detection. The aptasensor exhibited good linear responses between 40 and 200 nM NOD-R, with a detection limit as low as 167 pM. In addition, the aptasensor showed high specificity and a good reproducibility. The novel aptasensor may serve as an alternative to traditional analytical methods for the rapid and sensitive detection of NOD-R. However, the LOD of the aptasensor is still higher than with existing combined analytical methods. Also, the complicated structures and binding mechanism of NOD-R with the aptamer N13-T-O2 need to be further studied.

Conflicts of interest

All authors have declared that no competing interest exists.

Acknowledgments

This work was supported by Science and Technology Basic Work of Science and Technology (No. 2015FY111400) and China National Major Scientific and Technological Special Project for Significant New Drugs Development (No. 2018ZX09J18112).

References

View Article Online
DOI: 10.1039/C8AN00567B

1. S. Merel, D. Walker, R. Chicana, S. Snyder, E. Baures and O. Thomas, Environ. Int., 2013, 59, 303-327.
2. W. Carmichael, J. Eschedor, G. Patterson and R. Moore, Appl. Environ. Microbiol., 1988, 54, 2257-2263.
3. J. An and W. W. Carmichael, Toxicon, 1994, 32, 1495-1507.
4. B. W. Ibelings, L. C. Backer, W. E. Kardinaal and I. Chorus, Harmful Algae, 2015, 49, 63-74.
5. M. Agrawal, S. Yadav, C. Patel, N. Raipuria and M. K. Agrawal, Eur. J. Exp. Biol., 2012, 2, 321-336.
6. J. Chen, T. Yan, J. Xu, S. He, P. Zhao and X. Yan, J. Sep. Sci., 2012, 35, 1094-1101.
7. A. Gambaro, E. Barbaro, R. Zangrando and C. Barbante, Rapid Commun. Mass Spectrom., 2012, 26, 1497-1506.
8. T. Kaloudis, S. K. Zervou, K. Tsimeli, T. M. Triantis, T. Fotiou and A. Hiskia, J. Hazard. Mater., 2013, 263 Pt 1, 105-115.
9. Y. Shan, X. Shi, A. Dou, C. Zou, H. He, Q. Yang, S. Zhao, X. Lu and G. Xu, J. Chromatogr. A, 2011, 1218, 1743-1748.
10. J. S. Metcalf, S. G. Bell and G. A. Codd, Appl. Environ. Microbiol., 2001, 67, 904-909.
11. I. A. Samdal, A. Ballot, K. E. Lovberg and C. O. Miles, Environ. Sci. Technol., 2014, 48, 8035-8043.
12. A. D. Ellington and J. W. Szostak, Nature, 1990, 346, 818.
13. C. Tuerk and L. Gold, Science, 1990, 249, 505-510.
14. S. D. Jayasena, Clin. Chem., 1999, 45, 1628-1650.
15. L. Hou, L. Jiang, Y. Song, Y. Ding, J. Zhang, X. Wu and D. Tang, Microchimica Acta, 2016, 183, 1971-1980.
16. S. Gao, X. Zheng and J. Wu, Sensors Actuators B: Chem., 2017, 246, 169-174.
17. S. Gao, B. Hu, X. Zheng, Y. Cao, D. Liu, M. Sun, B. Jiao and L. Wang, Biosens. Bioelectron., 2016, 79, 938-944.
18. R. Elshafey, M. Siaj and M. Zourob, Biosens. Bioelectron., 2015, 68, 295-302.
19. R. Elshafey, M. Siaj and M. Zourob, Anal. Chem., 2014, 86, 9196-9203.
20. Z. Zhao, H. Chen, L. Ma, D. Liu and Z. Wang, Analyst, 2015, 140, 5570-5577.
21. F. Wang, S. Liu, M. Lin, X. Chen, S. Lin, X. Du, H. Li, H. Ye, B. Qiu, Z. Lin, L. Guo and G. Chen, Biosens. Bioelectron., 2015, 68, 475-480.
22. X. Du, D. Jiang, L. Dai, L. Zhou, N. Hao, J. Qian, B. Qiu and K. Wang, Biosens. Bioelectron., 2016, 81, 242-248.
23. G.-H. Yao, R.-P. Liang, X.-D. Yu, C.-F. Huang, L. Zhang and J.-D. Qiu, Anal. Chem., 2014, 87, 929-936.
24. L. Wang, R. Wang, F. Chen, T. Jiang, H. Wang, M. Slavik, H. Wei and Y. Li, Food Chem., 2017, 221, 776-782.
25. M. Santos-Cancel and R. J. White, Anal. Chem., 2017, 89, 5598-5604.
26. C. Bayrac, F. Eyidogan and H. Avni Oktem, Biosens. Bioelectron., 2017, 98, 22-28.
27. S. Gao, X. Zheng, B. Hu, M. Sun, J. Wu, B. Jiao and L. Wang, Biosens. Bioelectron., 2017, 89, 952-958.
28. F. Gao, Y. Qian, L. Du, Y. Zhang, D. Tang, D. Yang, Biosens. Bioelectron.,74, 2015, 483-490.
29. C. Wang, Y. Qian, Y. Zhang, S. Meng, S. Wang, Y. Li, F. Gao, Sensors Actuators B: Chem., 238, 2017, 434-440.
30. F. Gao, L. Du, Y. Zhang, F. Zhou, D. Tang, Biosens. Bioelectron., 86, 2016, 185-193.
31. D. Verzijl, T. Riedl, P. Parren and A. F. Gerritsen, Biosens. Bioelectron., 2017, 87, 388-395.
32. M. Zhang, X. Q. Jiang, H. N. Le, P. Wang and B. C. Ye, ACS Appl Mater Interfaces, 2013, 5, 473-478.
33. J. Concepcion, K. Witte, C. Wartchow, S. Choo, D. Yao, H. Persson, J. Wei, P. Li, B. Heidecker and W. Ma, Comb. Chem. High Throughput Screen., 2009, 12, 791-800.
34. Y. Hong, J. Muenzner, S. K. Grimm and E. V. Pletneva, J. Am. Chem. Soc., 2012, 134, 18713-18723.

View Article Online
DOI: 10.1039/C8AN00567B

35. G. Zhang, C. Li, S. Wu and Q. Zhang, Sensors Actuators B: Chem., 2018, 260, 42-47.
36. S. M. Taghdisi, N. M. Danesh, M. Ramezani, N. Ghows, S. A. Mousavi Shaegh and K. Abnous, Talanta, 2017, 166, 187-192.
37. X. Li, R. Cheng, H. Shi, B. Tang, H. Xiao and G. Zhao, J. Hazard. Mater., 2016, 304, 474-480.

View Article Online
DOI: 10.1039/C8AN00567B

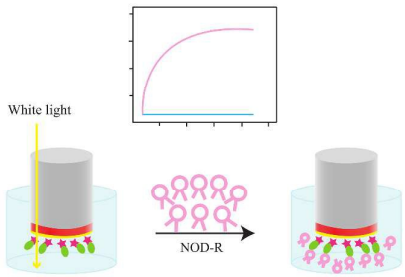

A novel label-free BLI aptasensor was developed for the rapid and sensitive detection of nodularin-R in water.